

Inelastic behavior of partially prestressed concrete under reversed cyclic loading

Kazuo Kobayashi, Susumu Inoue & Toshihiko Matsumoto
Kyoto University, Japan

ABSTRACT: Partially prestressed concrete (PPC) beams together with supplementary nontensioned mild steel, in which cracking is permitted under full working load conditions, were tested under reversed cyclic loading, and their fundamental inelastic behaviors connected with seismic resistance of structures were compared with those of reinforced concrete (RC) and fully prestressed concrete (PC) beams designed to have almost the same ultimate flexural strength.

1 INTRODUCTION

Partially prestressed concrete (PPC) has considerable freedom of design as compared to reinforced concrete (RC) and fully prestressed concrete (PC), and offers a good solution with regard to crack and deflection control. Therefore, the potential economic and serviceability advantages of PPC are being fully realized in construction practice. For their more extensive structural use, however, it is essential to make clear their fundamental inelastic behaviors when subjected to seismic loading.

In this study, a total of 28 beams including RC and PC beams are tested under three types of loading patterns in order to study their inelastic behaviors, in particular, after attainable maximum strength and also to find the effects of mechanical degree of prestress and tie reinforcement for lateral confinement.

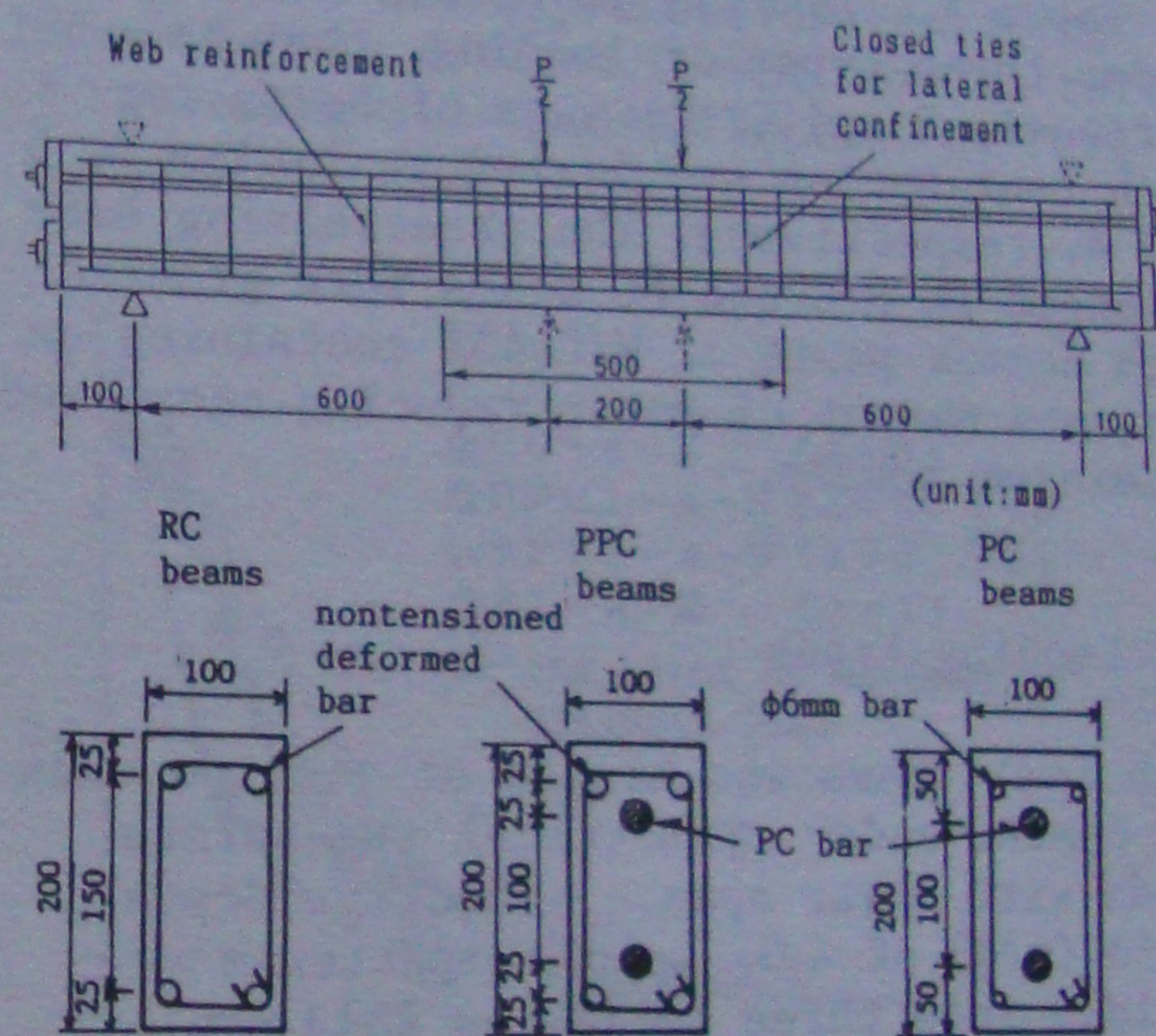


Fig.1 Details of tested beams

($\lambda=1$:PC) beams were also prepared for comparison. These four kinds of beam sections were symmetrically reinforced and designed to have approximately the same ultimate flexural strength among them.

In addition, supplementary reversed cyclic loading tests were also done on two kinds of unsymmetrically reinforced PPC beams having different λ -value (or ultimate flexural strength) between upper and lower part of section, that is, $\lambda=(\text{upper:}0.44, \text{lower:}0.56)$ and $(0.60, 0.78)$.

Each pair of two beams with or without $\phi 6\text{mm}$ rectangular closed tie ($f_{sy}=49\text{kgf/mm}^2$) for lateral confinement, each designated as R-type and N-type, were prepared for two types of reversed cyclic loading. These ties were arranged at the spacing of $s=d/4$ (d :

Dimensions of the beam specimen are shown in Fig.1. All of tested beams have a $10\text{cm} \times 20\text{cm}$ rectangular cross-section and length of 160cm .

Mechanical degree of prestress $\lambda (= A_p f_{py} / (A_p f_{py} + A_s f_{sy}))$, A_p, f_{py} : area and yield strength of prestressing steel, A_s, f_{sy} : those of nontensioned mild steel) was chosen as two levels of 0.44 and 0.78 for most of tested PPC beams. Conventionally reinforced ($\lambda=0$:RC) and fully prestressed

f_c' (kgf/cm ²)	Max Size of Aggregate (mm)	Slump (cm)	W/C (%)	s/a (%)	Unit contents (kg/m ³)				Admixture (cc/m ³)
					W	C	S	G	
400	15	5±1	53	42	175	330	767	1056	No.70 * 825

*water reducing agent

effective depth of section) within an expected plastic hinge zone of 50cm length over a mid-span of beam on the basis of the provisions drafted by the New Zealand Concrete Design Code Committee (1976). And, the vertical rectangular stirrups of $\phi 6$ mm were provided as web reinforcement in the remaining part of span, the amount of which was determined by taking into account the shear resistance of concrete according to the JSCE PC Standard Code (1978).

The design compressive strength of concrete was $f_c' = 400 \text{ kgf/cm}^2$ throughout the tested beams and its mix proportion is given in Table 1. Totally 28 beams were tested under three types of loading, that is, Series-A, B and C. Details of beams for each test series are listed in Tables 2, 3 and 4, respectively. The prestressing bars arranged in PPC and PC beams were grouted with cement paste of W/C=45% containing an adequate amount of water reducing agent and aluminium powder.

2.2 Loading types

Each test beams was hinged at its two ends and tested under symmetrical two-points loads with shear span - effective depth ratio (a/d) of 4.0. Loading patterns are divided into three series as follows.

(1) Series-A (unidirectional cyclic loading)

Series-A tests were done in order to obtain the basic data for following Series-B and C tests. Loading sequence of Series-A tests is shown schematically in Fig.2-(1). The beams were fully unloaded at each repetition when the load attained the compression fiber strain of mid-span section

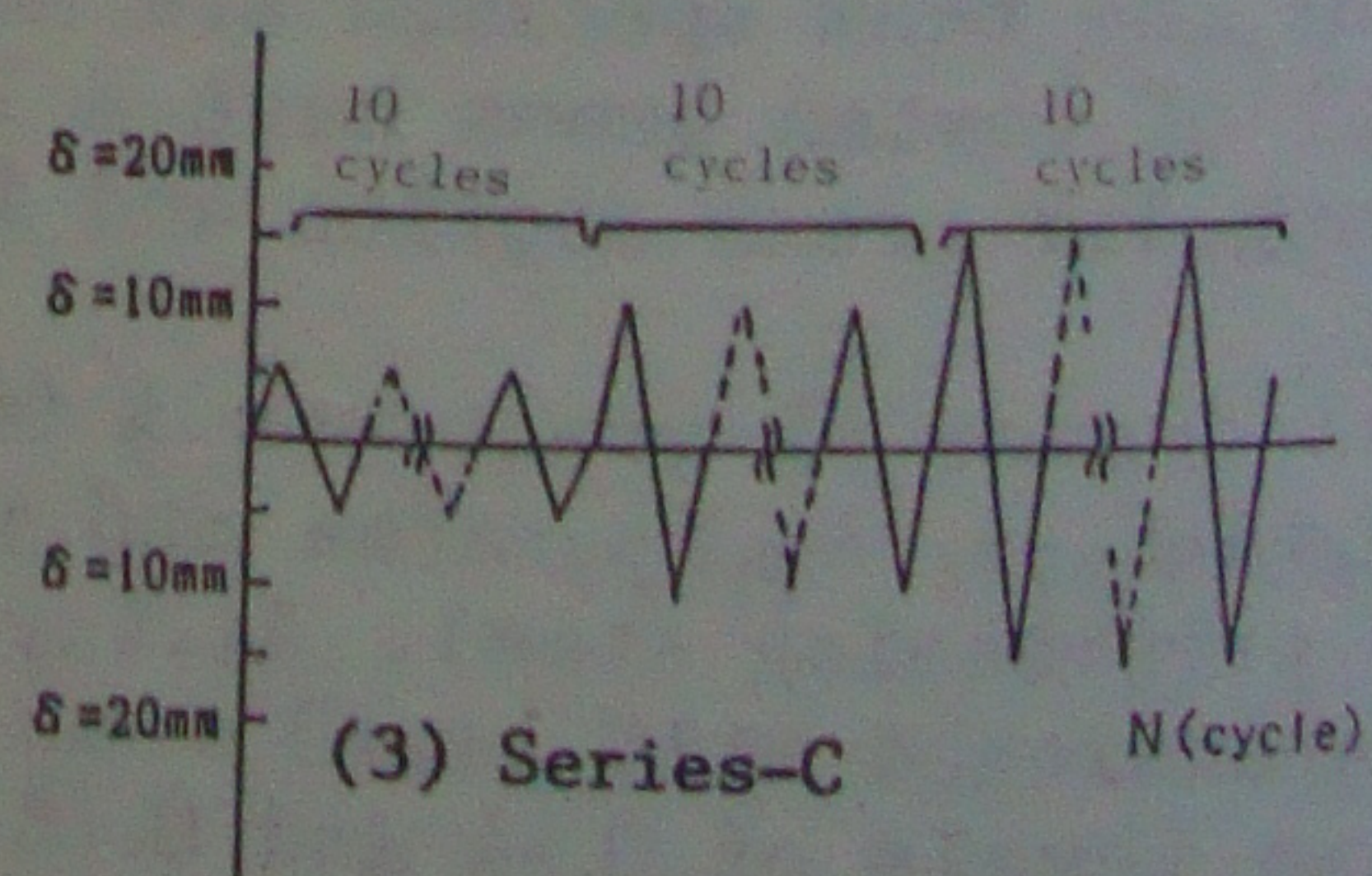
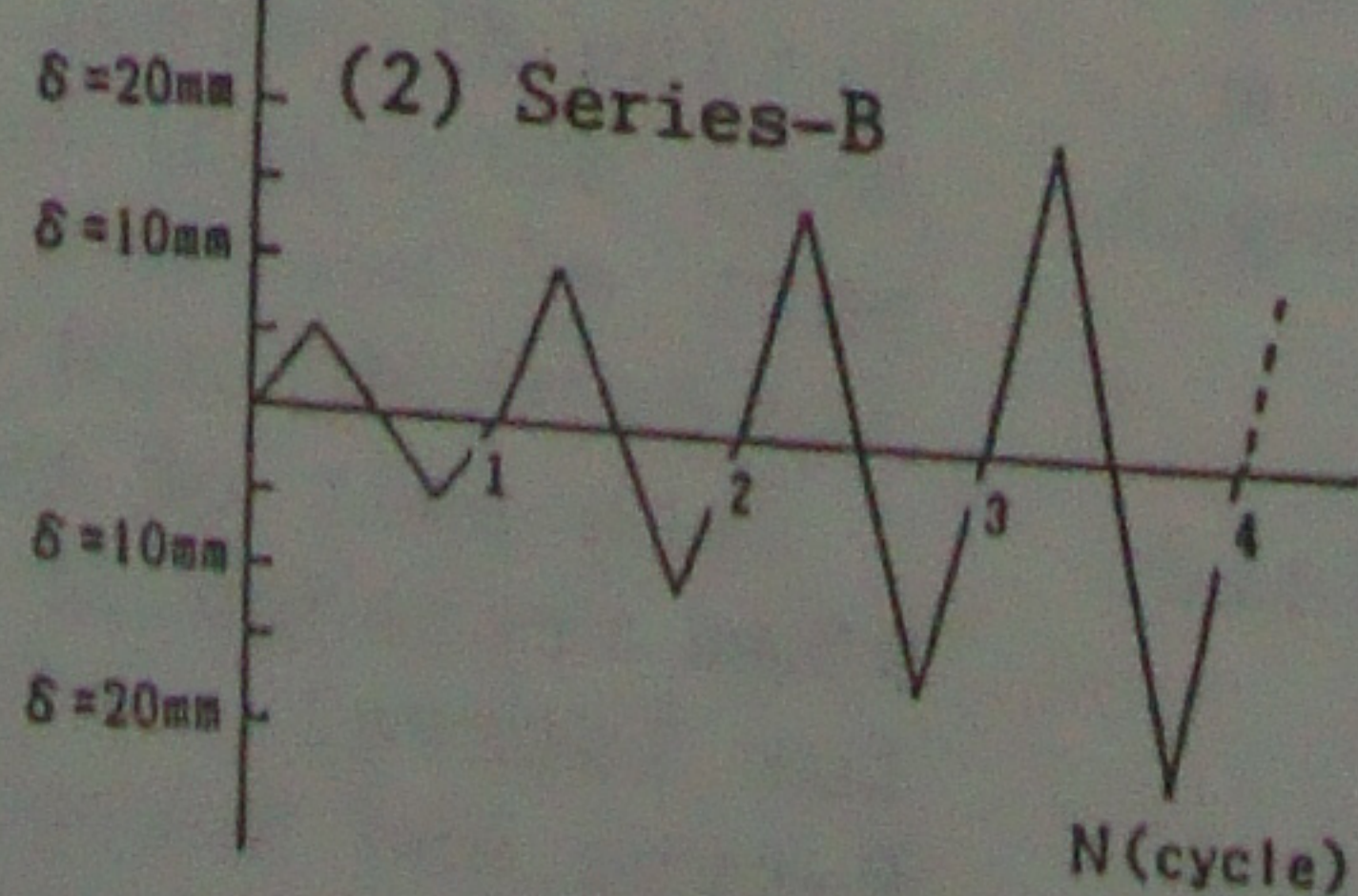
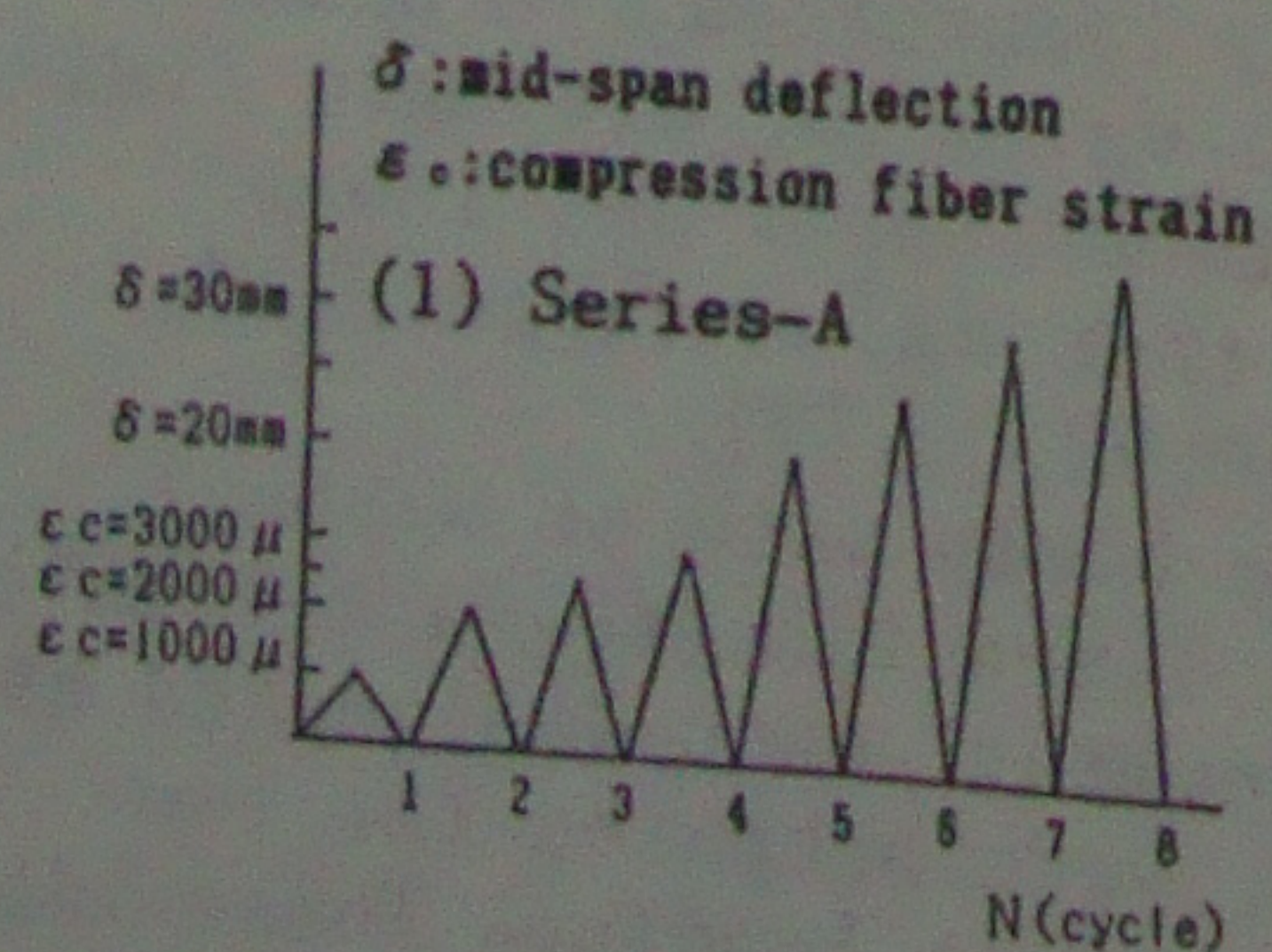


Fig.2 Details of loading patterns

(ϵ_c) of 0.001, 0.002, 0.0025, 0.003, the maximum ultimate load (P_u) and also the levels corresponding to the mid-span deflection of $\delta = 20 \text{ mm} (\theta = 0.029)$, $\delta = 25 \text{ mm} (\theta = 0.036)$, $\delta = 30 \text{ mm} (\theta = 0.043)$... in the falling branch region after P_u , in which θ indicates the rotation angle ($\theta = 2\delta/l$, l:span length).

(2) Series-B (reversed bidirectional cyclic loading without load repetitions)

As shown in Fig.2-(2), each one cycle of load reversal was given at gradually increased deflection amplitudes of $\delta = \pm \delta_y (\theta = \pm 0.007) \rightarrow \pm 2\delta_y \rightarrow \pm 3\delta_y \dots$ ($\delta_y = 5 \text{ mm}$: chosen in these tests as the mid-span deflection at first yielding of RC beams).

(3) Series-C (reversed bidirectional cyclic loading with load repetitions)

As shown in Fig.2-(3), reversed cyclic loading with load repetitions of each ten cycles was applied at several levels of deflection amplitude of $\delta = \pm \delta_y (\theta = \pm 0.007) \rightarrow \pm 2\delta_y \rightarrow \pm 3\delta_y \dots$

3 RESULTS OF TESTS AND DISCUSSIONS

3.1 Series-A

All beams in Series-A tests failed finally in flexure. In Table 2 are shown their measured flexural cracking loads (P_{cr}) and maximum ultimate loads (P_u) together with the calculated ultimate ones (P_u'). P_u' is calculated by the conventional ultimate strength theory using rectangular stress block equal to 0.85 times of cylinder concrete strength (f_c') and yield strength of steels (f_{sy} , f_{py}). Ductility factor (μ) in Table 2 is defined in the term of two

Table 2 Kinds of beams and test results (Series-A)

Specimens	Mechanical Degree of Prestress	Steel * Index	Tie Spacing	A _s	A _p ***	Prestress σ _p (kgf/cm ²)	Flexural Cracking Load Per (tonf)	Maximum Load	Ultimate (tonf)	Ductility Factor μ
	λ	q	S					Measured P _u	Calculated P _u *	
RC-A-N	0	0.184	∞	2D16	—	—	2.25	9.74	7.64	16.50
PPC1-A-N	0.440	0.231	∞	2D13	φ9.2-B	44	4.02	9.97	8.13	6.84
PPC2-A-N	0.780	0.252	∞	2D10	φ13-A	98	4.09	9.47	7.90	3.43
PC-A-N	1	0.276	∞	(2φ6**)	φ13-C	132	5.52	9.00	8.37	2.17

* $q = A_p \cdot f_{py} / (b \cdot d_p \cdot f_c') + A_s \cdot f_{sy} / (b \cdot d_s \cdot f_c')$
 ** used for arrangement of stirrups and ties
 *** φ9.2-B: $f_{py} = 114 \text{ kgf/mm}^2$, φ13-A: $f_{py} = 94 \text{ kgf/mm}^2$, φ13-C: $f_{py} = 125 \text{ kgf/mm}^2$

mid-span deflections at $0.9P_u$ on the ascending and falling branch curves given by an envelope of the load-deflection hysteresis.

Flexural cracking strength is clearly found to increase with increasing λ-value, when reinforced to have approximately the same maximum ultimate strength.

Fig.3 shows the measured load-deflection (P-δ) hysteresis of Series-A beams together with each theoretical P-δ envelope curve, which was calculated by modifying

the stress-strain relationships of constitutive materials proposed by Park et al (1980, 1973) as illustrated in Fig.4. As seen in Fig.3 and Table 1, beam ductility decreases with increasing λ-value. Theoretical P-δ envelope curve of each beam coincides well with the measured one.

On the other hand, the elastic recoveries are compared among four tested beams in Fig.5, which are expressed by restoring index (α) as defined in the term of ratio of restoring mid-span deflection at full

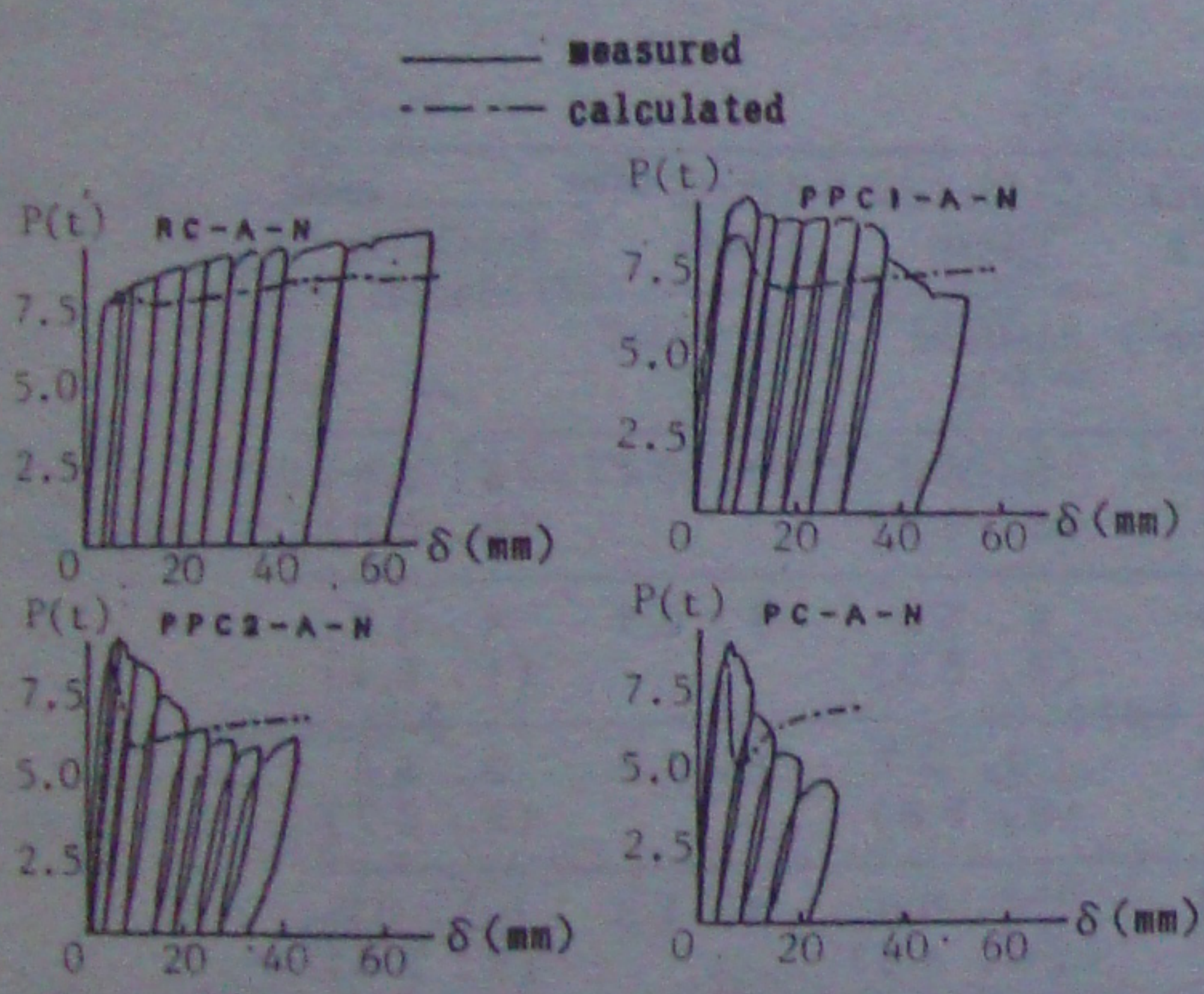


Fig.3 Load-deflection hysteresis loops (Series-A)

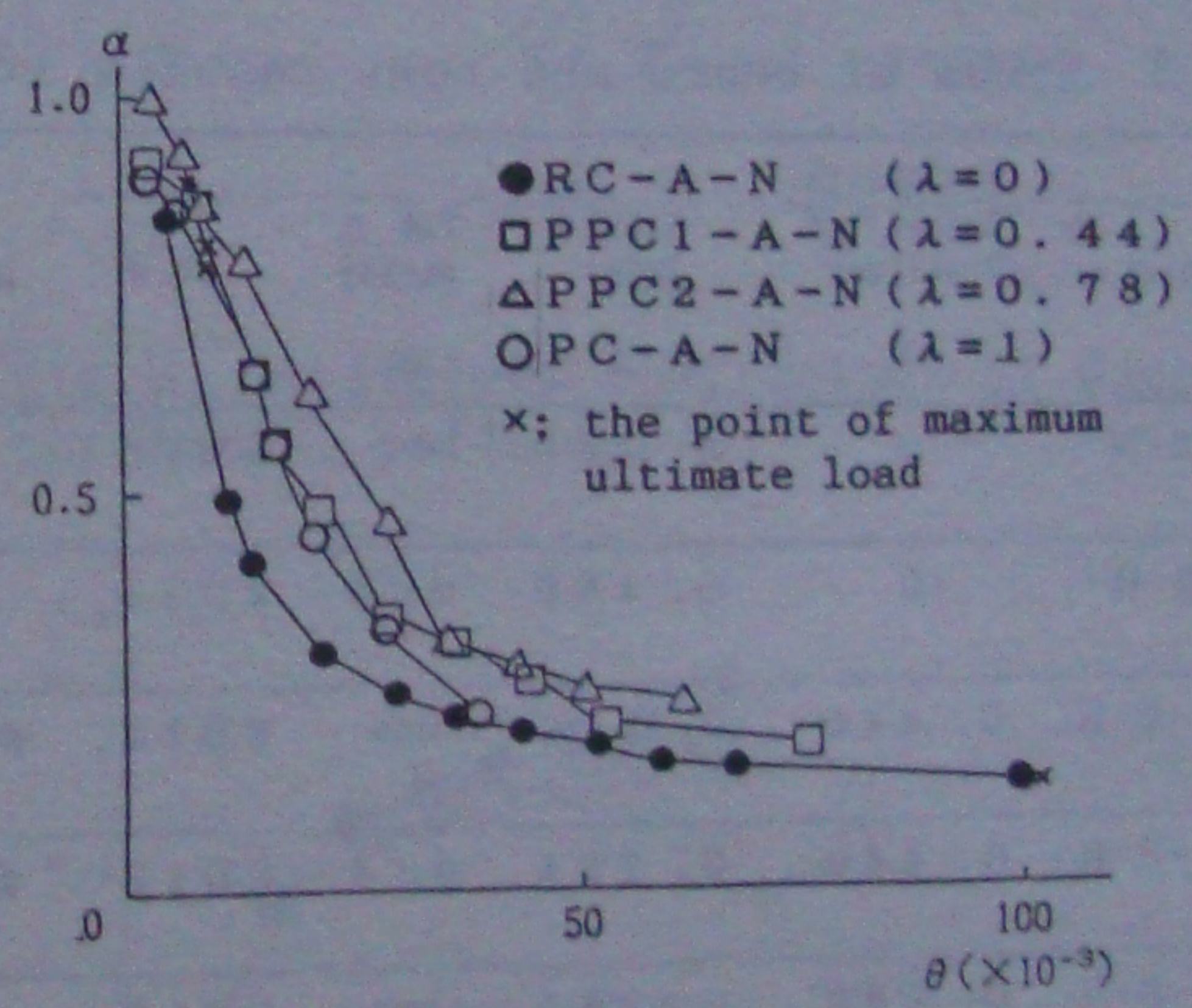
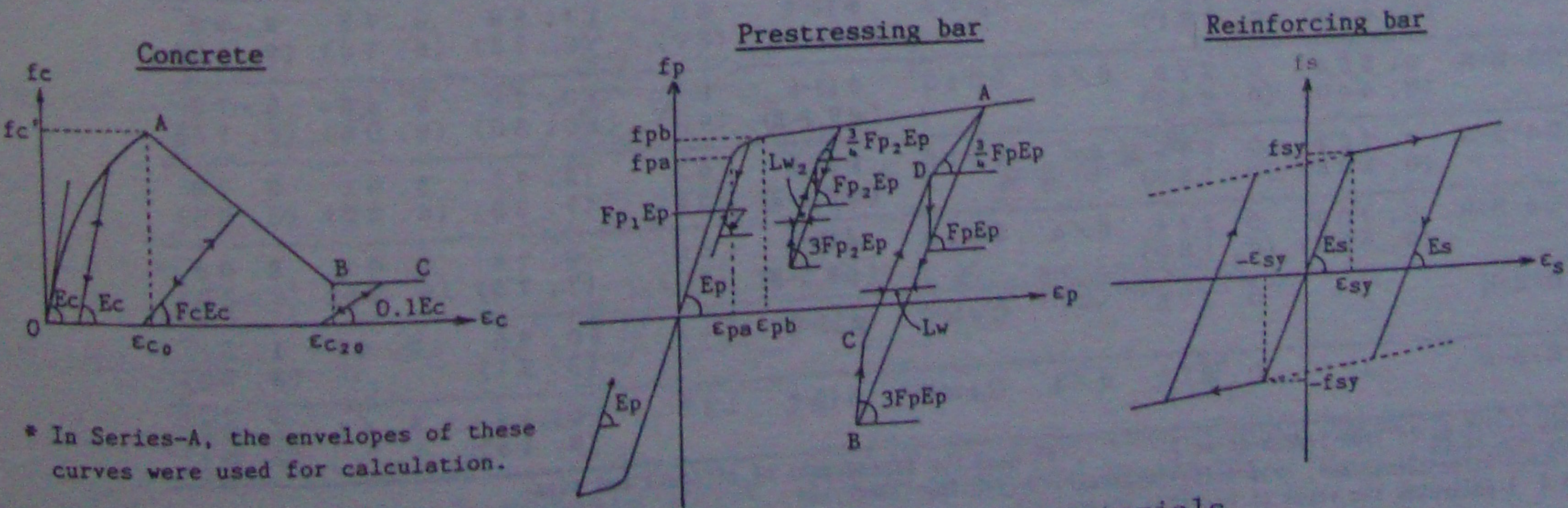


Fig.5 Elastic recovery expressed by restoring index (Series-A)



* In Series-A, the envelopes of these curves were used for calculation.

Fig.4 Modified stress-strain relations of constitutive materials

unloading to total one. Even in the PPC beam having relatively low λ -value of 0.44, the index α is well in excess of 0.9 before the maximum ultimate load ($\theta < 0.01$). Within the falling branch region after that, however, α commences to decrease rapidly irrespective of magnitude of λ .

3.2 Series-B

All of PPC beams as well as PC ones failed finally in flexure under reversed cyclic loading as done in Series-B tests. On the other hand, RC beams showed brittle shear failure due to significant reduction in effectiveness of concrete shear resistance mechanism after the formation of X-shaped diagonal shear cracks at $\delta = \pm 4\delta_y$, although failed in flexure in a more ductile manner under unidirectional loading.

Table 3 shows the measured maximum ultimate loads (P_u) together with theoretical ones (P_u') estimated by the same method as done for Series-A beams. It is indicated in Table 3 that the measured maximum ultimate load of any beam including RC beams, however, is well in excess of the theoretical

one even under the reversed cyclic loading. Fig.6 shows the measured load-deflection ($P-\delta$) hysteresis of Series-B beams together with the theoretical $P-\delta$ envelope curves obtained by the same method as applied for Series-A and also the measured $P-\delta$ envelope curve of each corresponding Series-A beam. And then, in Fig.7 are shown some examples of the moment-curvature ($M-\phi$) hysteresis loops measured within the maximum moment span together with the theoretical ones calculated on the basis of stress-strain relationships of constitutive materials as already illustrated in Fig.4.

Load carrying capacity of N-type beams without tie reinforcement reduces rapidly once the cyclic load exceeds P_u . This strength reduction becomes more remarkable in beams having higher λ -value. However, it is clearly indicated in Table 3 and Fig.6 that the ductility of PPC and PC beams which failed finally in flexure can be improved remarkably by arranging tie reinforcement. Comparing the measured $P-\delta$ envelopes of corresponding two beams between Series-B and Series-A tests, the reduction in load carrying capacity is found to commence somewhat earlier in the former than in the latter.

Table 3 Kinds of beams and test results (Series-B)

Specimens	Mechanical Degree of Prestress	Steel Index	Tie spacing	A_s	A_p ***	Prestress σ_p (kgf/cm ²)	Maximum Ultimate ****		Ductility Factor μ
	λ	q	s				Load Measured P_u	(tonf) Calculated P_u'	
RC-B-N	0	0.180	∞	2D16	—	—	8.66 (8.61)	7.67	5.76 (2.60)
RC-B-R	0	0.180	d/4	2D16	—	—	9.50 (9.50)	7.67	4.02 (1.84)
PPC1-B-N	0.440	0.231	∞	2D13	$\phi 9.2-B$	49	10.27 (9.56)	8.13	3.52 (5.67)
PPC1-B-R	0.440	0.231	d/4	2D13	$\phi 9.2-B$	48	12.00 (10.44)	8.13	10.00 (7.25)
PPC2-B-N	0.780	0.264	∞	2D10	$\phi 13-A$	91	9.64 (9.13)	8.01	3.83 (4.03)
PPC2-B-R	0.780	0.264	d/4	2D10	$\phi 13-A$	93	9.88 (9.60)	8.01	7.73 (6.33)
PPC3-B-N	0.564 (0.440)	0.303 (0.231)	∞	2D13	$\phi 13-A$ ($\phi 9.2-B$)	90 (39)	11.56 (9.73)	9.75 (8.13)	2.66 (2.73)
PPC3-B-R	0.564 (0.440)	0.318 (0.243)	d/4	2D13	$\phi 13-A$ ($\phi 9.2-B$)	98 (40)	10.75 (10.60)	9.65 (8.08)	5.73 (5.73)
PPC4-B-N	0.708 (0.596)	0.264 (0.189)	∞	2D10	$\phi 13-A$ ($\phi 9.2-B$)	93 (39)	9.75 (7.25)	8.01 (6.25)	2.79 (3.56)
PPC4-B-R	0.708 (0.596)	0.264 (0.189)	d/4	2D10	$\phi 13-A$ ($\phi 9.2-B$)	89 (40)	9.78 (7.75)	8.01 (6.25)	8.08 (7.50)
PC-B-N	1	0.276	∞	(2 $\phi 6$ **)	$\phi 13-C$	111	10.69 (8.81)	8.41	1.53 (2.20)
PC-B-R	1	0.276	d/4	(2 $\phi 6$ **)	$\phi 13-C$	115	10.13 (9.13)	8.41	2.09 (3.64)

* $q = A_p \cdot f_{py} / (b \cdot d_p \cdot f_c') + A_s \cdot f_{sy} / (b \cdot d_s \cdot f_c')$
 ** used for arrangement of stirrups and ties
 *** $\phi 9.2-B: f_{py} = 114 \text{ kgf/mm}^2$, $\phi 13-A: f_{py} = 94 \text{ kgf/mm}^2$, $\phi 13-C: f_{py} = 125 \text{ kgf/mm}^2$
 **** () indicates the value of negative direction

In RC beams, a significant pinching effect in P- δ hysteresis loops is observed due to extensive X-shaped diagonal shear cracks at

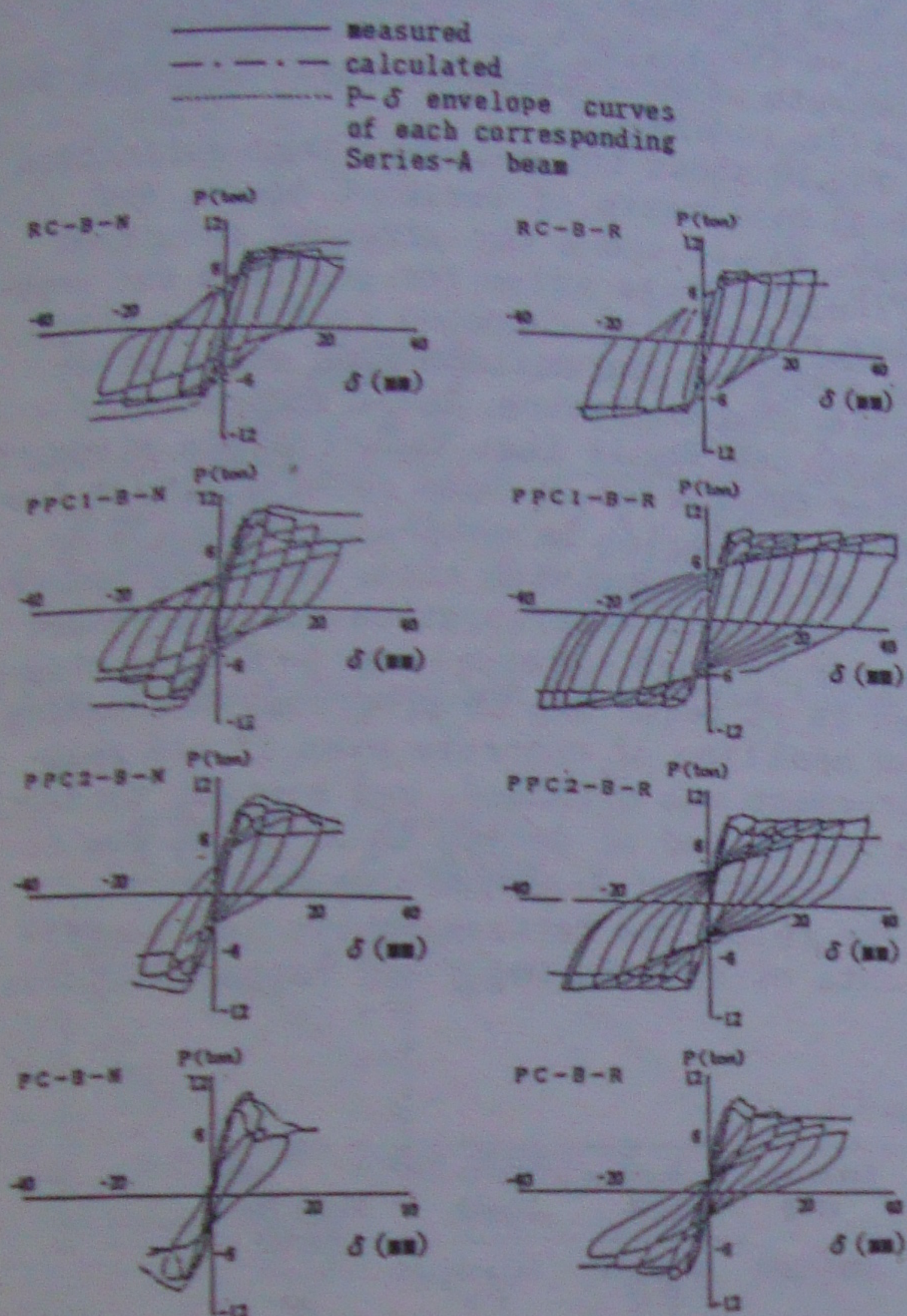


Fig.6 Load-deflection hysteresis loops (Series-B)

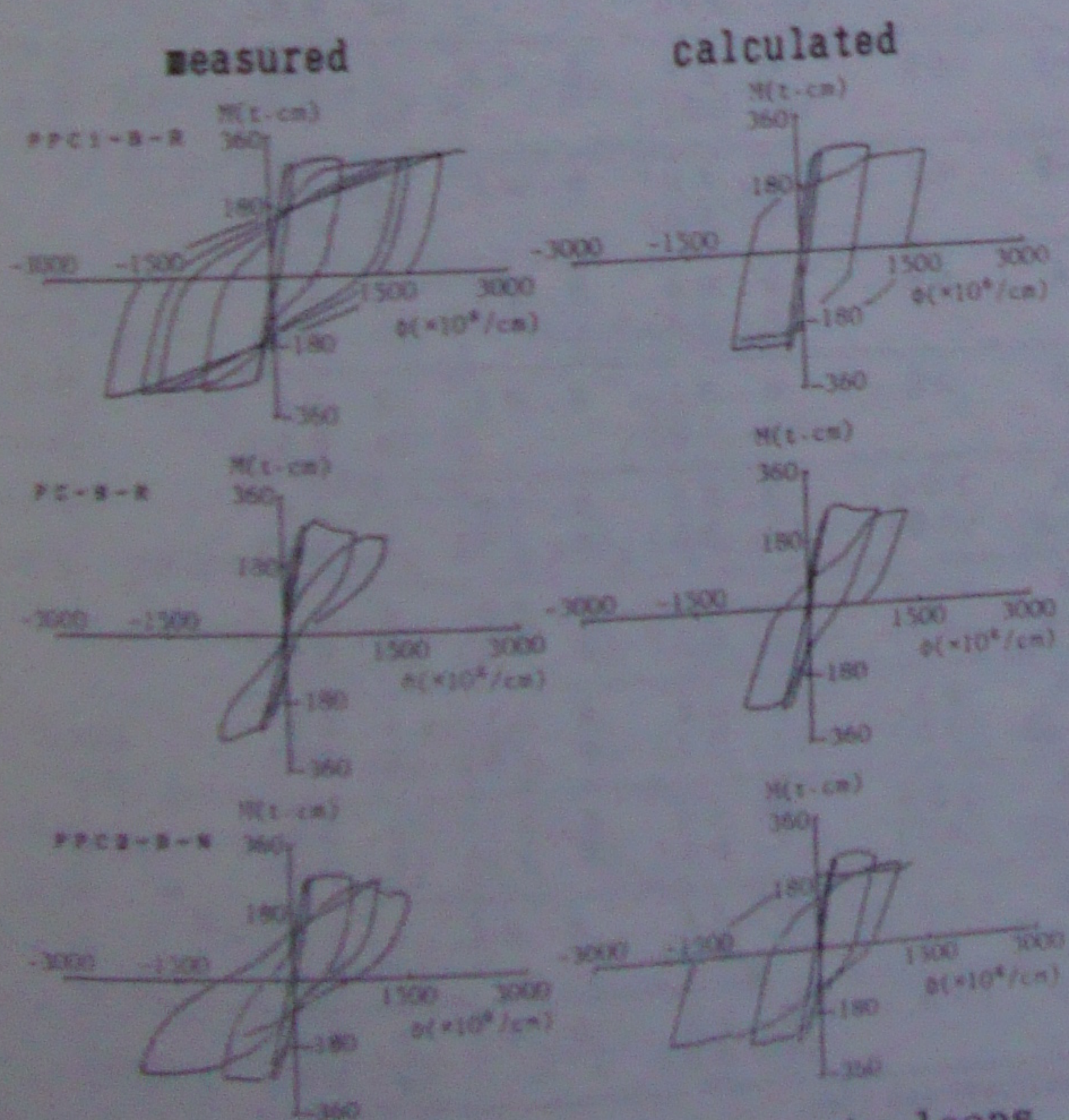


Fig.7 Moment-curvature hysteresis loops (Series-B)

about $\delta = \pm 6\delta_y$ ($\theta = \pm 0.043$), although stable before $\delta = \pm 5\delta_y$ ($\theta = \pm 0.031$).

As shown in Fig.7, the M- ϕ hysteresis loop for any type of PPC beams can be well estimated by the above mentioned analysis.

The equivalent coefficients of damping (h_{eq}) obtained from the measured P- δ hysteresis loops of Series-B beams are shown in Fig.8. The h_{eq} -value increases with increase in the deflection amplitude or rotation angle (θ). When compared at the same θ -value of $\theta < 0.021$, the h_{eq} -value of RC beam is considerably larger than that of PPC beam, but commences to decrease due to pinching effect after $\theta \geq 0.021$. It is observed in the PPC and PC beams that the h_{eq} -value of N-type tends to increase more rapidly with increase in θ -value and to be higher

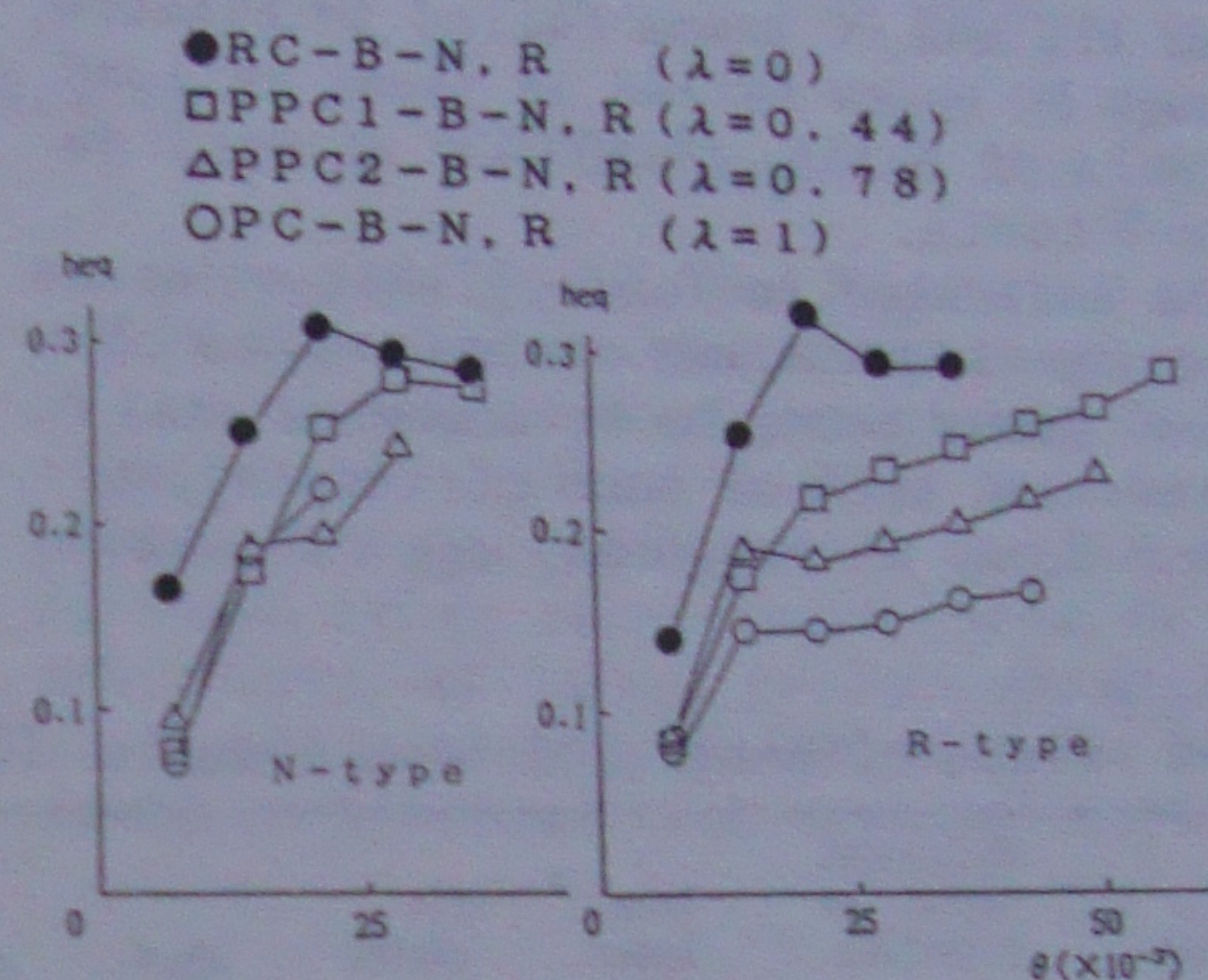


Fig.8 Equivalent coefficient of damping (Series-B, effect of λ)

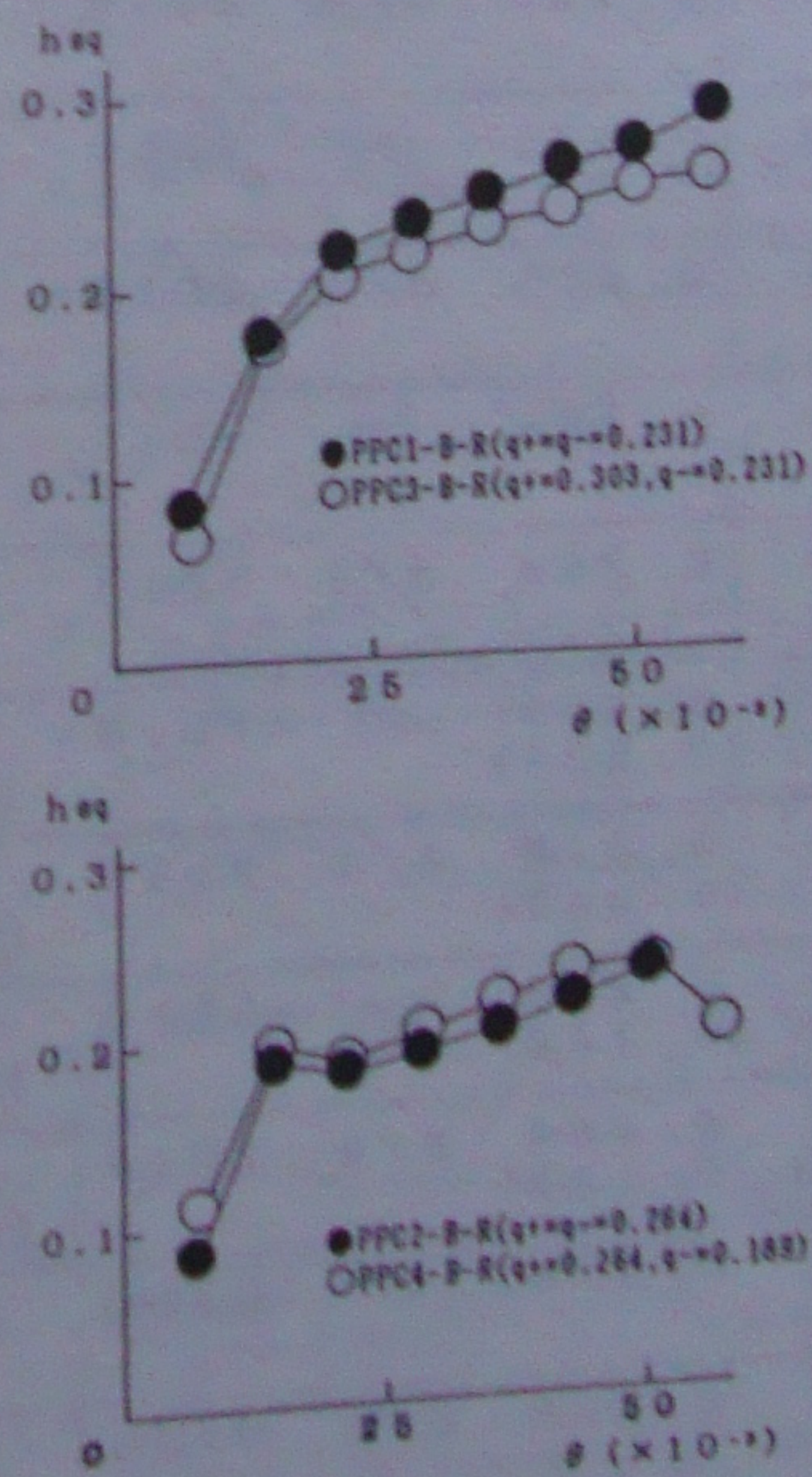


Fig.9 Comparison of h_{eq} between unsymmetrically and symmetrically reinforced beams (Series-B)

than that of R-type. However, a significant difference cannot be recognized in the h_{eq} -values between RC beams of N-type and R-type because of extensive shear cracks irrespective of beam types.

Comparing the h_{eq} -value of unsymmetrically reinforced PPC beam with that of symmetrically reinforced one, both of which have the same degree of prestress (λ) or steel index (q) ($= (p_s f_{sy} + p_p f_{py}) / f_c'$) in one side of section, as shown in Fig.9 the former is somewhat smaller than the latter when another side of section is reinforced with higher λ or q -value (PPC3 vs PPC1), while larger in the opposite case (PPC4 vs PPC2).

3.3 Series-C

All of PPC and PC beams failed in flexure, although RC beams failed in shear at load reversals of $\delta = \pm 6\delta_y$ ($\theta = \pm 0.043$) as well as Series-B tests.

It is indicated in Table 4 that an attainable negative maximum ultimate load of Series-C beams tends to be somewhat small compared with that of each corresponding Series-B beam, although any one is well in

excess of theoretical value.

The results of Series-B and Series-C tests confirm that the introduction of prestress of about 50kgf/cm² to the beam, as done in tested PPC beams of $\lambda = 0.44$, is very effective for preventing the degradation of concrete shear resistance under the reversed cyclic loading.

Fig.10 shows the measured load-deflection ($P-\delta$) hysteresis of Series-C beams. And then, Fig.11 shows the strength reduction (P/P_{max} : average value for positive and negative sides) with repeated cycles, in which P_{max} denotes the maximum load at a given deflection amplitude. It is indicated in Fig.10 and Fig.11 that reduction in strength after ten cycles of load reversals, for instance, at $\delta = \pm 4\delta_y$ is only less than 10% in all of PPC beams with ties. However, remarkable strength deterioration with increased number of load reversals at $\delta = \pm 3\delta_y$ is observed in PC beams due to progressive crushing and spalling of concrete even if tie reinforcement was arranged, and similar tendency is recognized at $\delta = \pm 4\delta_y$ in RC beams due to development of X-shaped cracks.

The relations between equivalent coefficients of damping (h_{eq}) and repeated cycles

Table 4 Kinds of beams and test results (Series-C)

Specimens	Mechanical Degree of Prestress λ	Steel * Index q	Tie spacing s	A_s	A_p ***	Prestress σ_p (kgf/cm ²)	Maximum Ultimate ****		Ductility Factor μ
							Load Measured P_u	(tonf) Calculated P_u'	
RC-C-N	0	0.180	∞	2D16	—	—	8.60 (8.38)	7.67	2.79 (2.77)
RC-C-R	0	0.180	d/4	2D16	—	—	8.81 (8.31)	7.67	3.57 (5.88)
PPC1-C-N	0.440	0.231	∞	2D13	$\phi 9.2-B$	46	10.31 (9.85)	8.13	2.38 (2.67)
PPC1-C-R	0.440	0.231	d/4	2D13	$\phi 9.2-B$	47	10.49 (9.49)	8.13	4.00 (4.56)
PPC2-C-N	0.780	0.264	∞	2D10	$\phi 13-A$	88	9.64 (8.94)	8.01	1.71 (2.26)
PPC2-C-R	0.780	0.264	d/4	2D10	$\phi 13-A$	92	9.81 (9.19)	8.01	6.94 (5.68)
PPC3-C-N	0.564 (0.440)	0.303 (0.231)	∞	2D13	$\phi 13-A$ ($\phi 9.2-B$)	100 (38)	12.63 (9.53)	9.75 (8.13)	1.92 (2.84)
PPC3-C-R	0.564 (0.440)	0.318 (0.243)	d/4	2D13	$\phi 13-A$ ($\phi 9.2-B$)	104 (43)	12.51 (9.63)	9.65 (8.08)	3.64 (4.80)
PPC4-C-N	0.708 (0.596)	0.264 (0.189)	∞	2D10	$\phi 13-A$ ($\phi 9.2-B$)	91 (35)	11.03 (7.01)	8.01 (6.25)	1.99 (2.76)
PPC4-C-R	0.708 (0.596)	0.264 (0.189)	d/4	2D10	$\phi 13-A$ ($\phi 9.2-B$)	108 (33)	9.44 (7.51)	8.01 (6.25)	5.24 (6.00)
PC-B-N	1	0.276	∞	(2 $\phi 8$ *)	$\phi 13-C$	111	10.44 (8.81)	8.41	1.51 (1.84)
PC-B-R	1	0.276	d/4	(2 $\phi 8$ *)	$\phi 13-C$	115	10.38 (9.63)	8.41	1.59 (2.26)

* $q = A_p f_{py} / (b d_p f_c') + A_s f_{sy} / (b d_s f_c')$ ** used for arrangement of stirrups and ties
 *** $\phi 9.2-B: f_{py} = 114 \text{ kgf/mm}^2$, $\phi 13-A: f_{py} = 94 \text{ kgf/mm}^2$, $\phi 13-C: f_{py} = 125 \text{ kgf/mm}^2$
 **** () indicates the value of negative direction

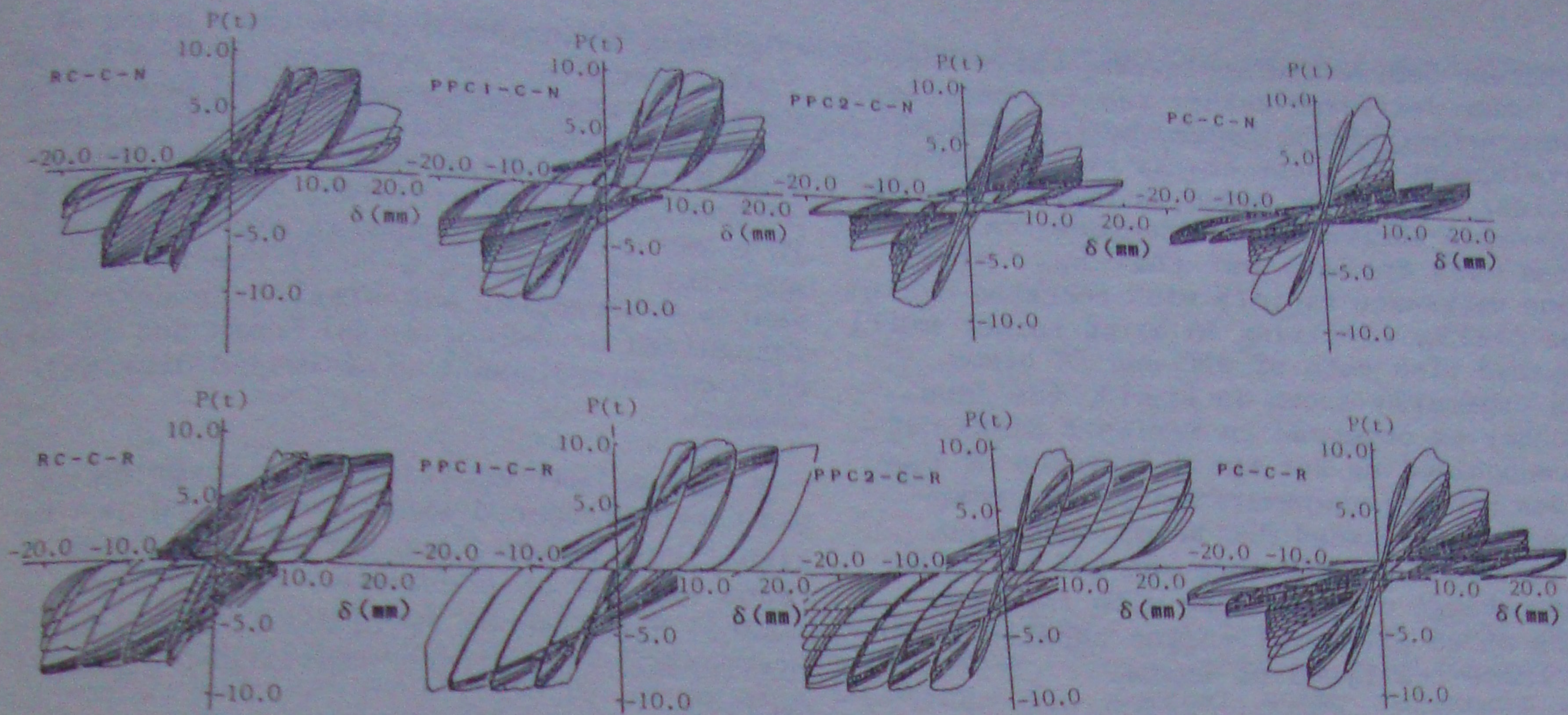


Fig.10 Load-deflection hysteresis loops (Series-C)

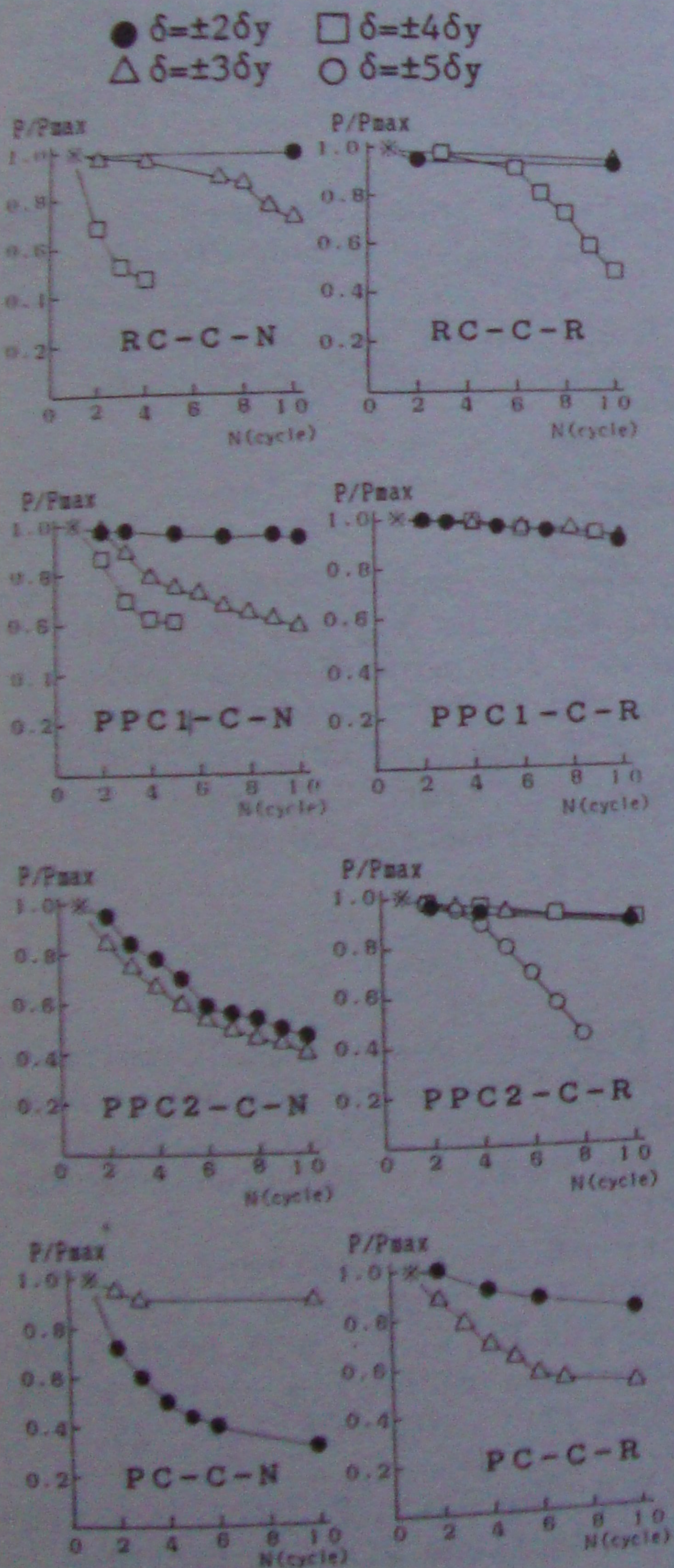


Fig.11 Strength reduction with repeated cycles (Series-C)

are shown in Fig.12. The h_{eq} -value of PPC and PC beams decreases somewhat abruptly at the second cycle of relatively small deflection amplitude of $\delta = \pm 2\delta_y$, but any marked change of h_{eq} -value can not be observed up to tenth cycle after third cycle. On the other hand, at larger deflection amplitude of $\delta \geq \pm 4\delta_y$, the h_{eq} -value of these beams tends to increase with repeated cycles at a

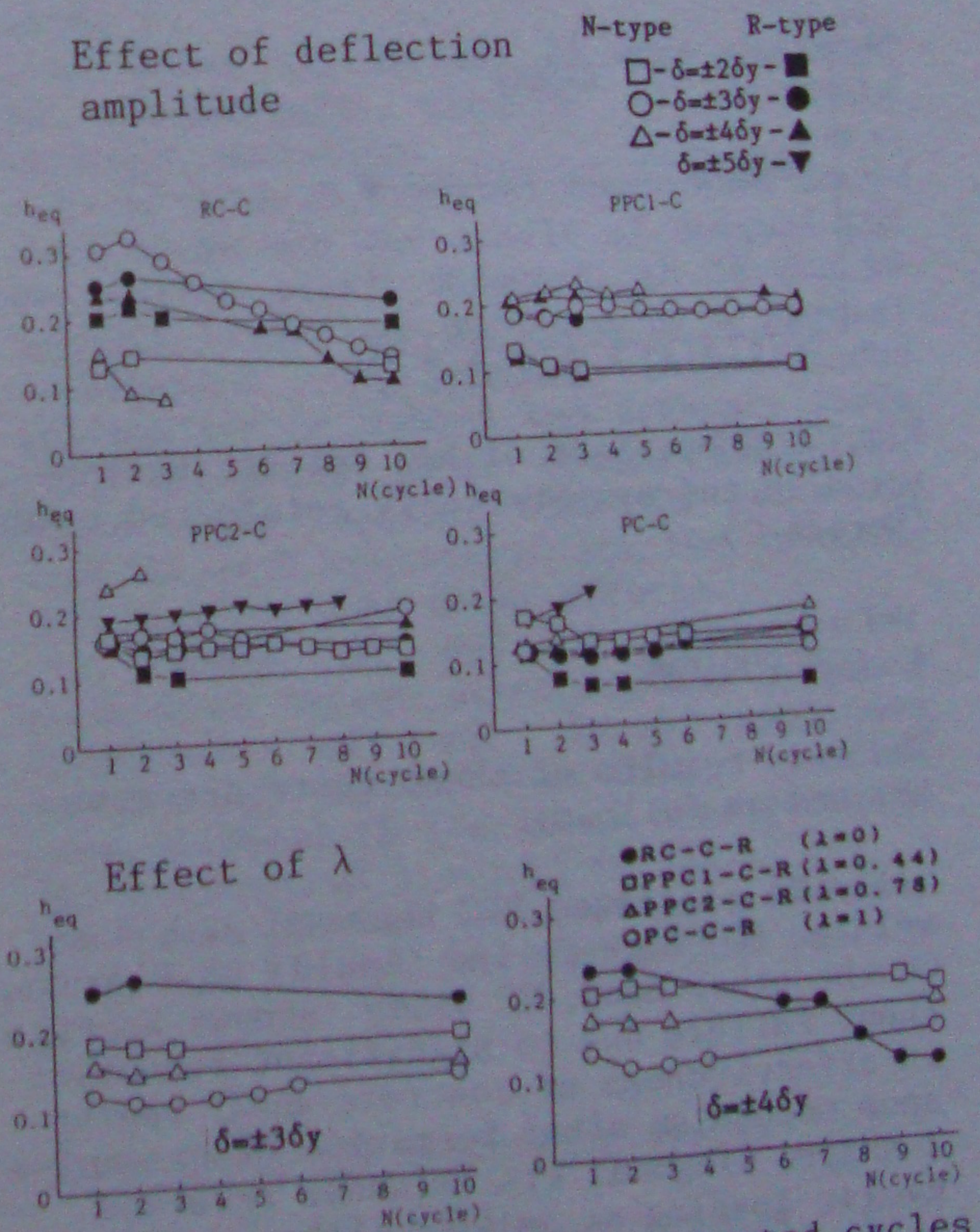


Fig.12 Changes of h_{eq} with repeated cycles (Series-C)

constant deflection amplitude, while that of RC beams decreases rather rapidly because of the pinching effect caused by the gradual development of shear cracks with repeated cycles. It is also found in Fig.12 that the h_{eq} -value increases with decrease in λ -value when $\delta \leq 3\delta_y$, but that h_{eq} of RC beams decreases rapidly with repeated cycles when $\delta > 3\delta_y$, resulting in being rather small compared with both of PPC and PC beams.

As typically shown in Fig.13, the same tendency as observed in Series-B tests can be recognized as for the difference of h_{eq} -values between unsymmetrically and symmetrically reinforced PPC beams. And also, any remarkable difference can not be found in the change of h_{eq} -value with repeated cycles at an given deflection amplitude between these two types of beams.

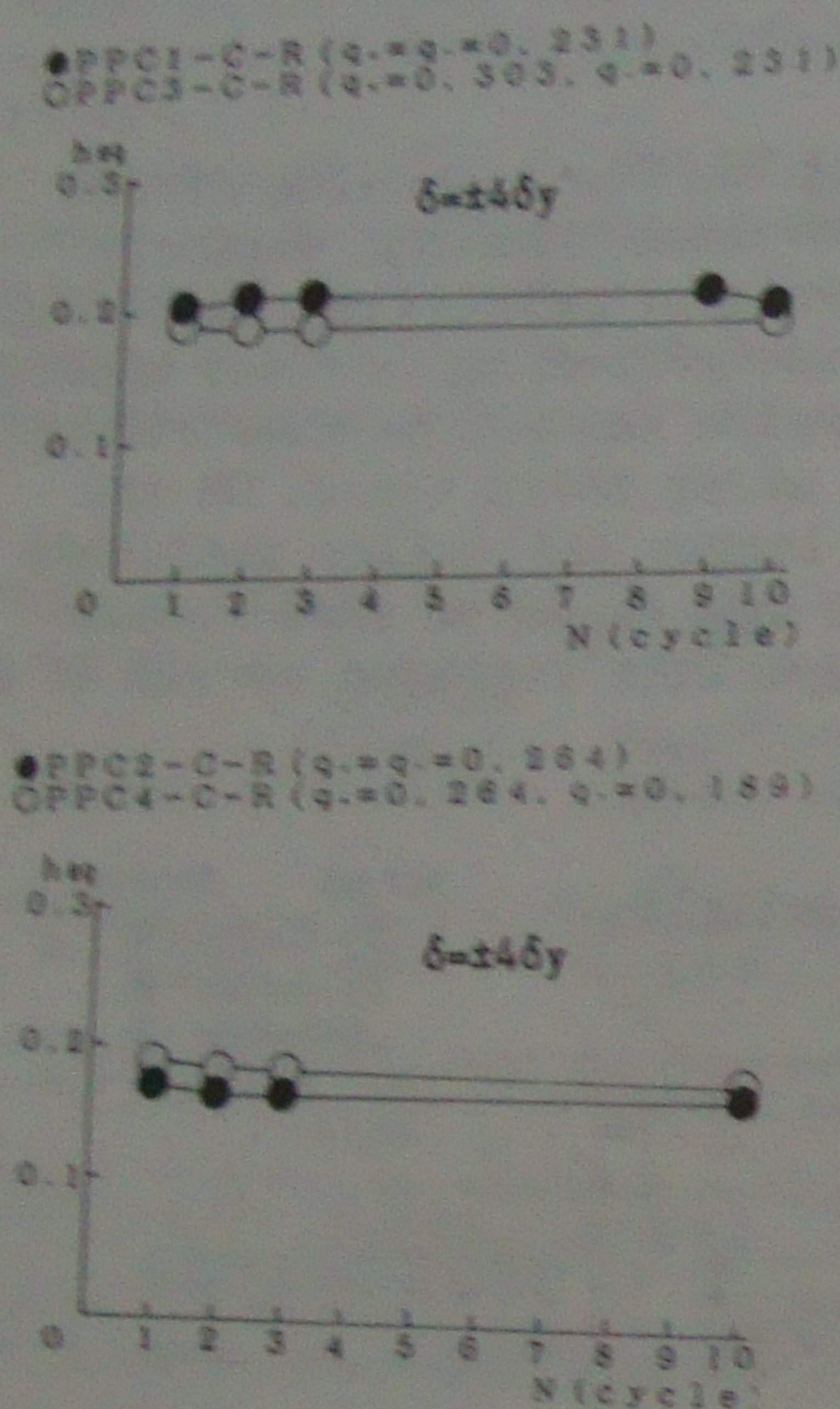


Fig.13 Comparison of h_{eq} between unsymmetrically and symmetrically reinforced beams (Series-C)

4 CONCLUSIONS

The main results of these tests are summarized as follows:

1. All of tested PPC beams of $\lambda \geq 0.44$ as well as PC beams failed finally in flexure. On the other hand, RC beams showed brittle shear failure due to significant reduction in effectiveness of concrete shear resistance mechanism after formation of extensive X-shaped diagonal cracks under reversed cyclic loading at $\delta = \pm 4\delta_y$, although failed in flexure under unidirectional loading.

2. Loss in strength after ten cycles of load reversals, for instance, at $\delta = \pm 4\delta_y$ was only less than 10% in all of PPC beams with tie reinforcement. However, remarkable strength deterioration with increased number of load reversals at $\delta = \pm 3\delta_y$ was observed in PC beams due to progressive crushing and spalling of concrete even if tie reinforcement was arranged, and similar tendency was recognized at $\delta = \pm 4\delta_y$ in RC beams due to significant development of X-shaped diagonal cracks.

3. Equivalent coefficient of damping as well as dissipated energy was found to be significantly affected not only by beam types (degree of prestress, tie reinforcement) but also by reversed cyclic loading conditions (deflection amplitude, repeated cycles).

4. Moment-curvature hysteresis loops for any types of PPC beams could be well estimated by taking into account the stress-strain relationship of constitutive materials and confinement effect of tie reinforcement.

5. The results of these fundamental tests implied that the inelastic behaviors of PPC beam under reversed cyclic loading as experienced with earthquake action was favourable in comparison with RC or PC beam.

ACKNOWLEDGMENT

The authors wish to express their appreciation to prof. emeritus Kiyoshi Okada at Kyoto University for providing valuable advices. And, the authors are also deeply grateful to colleagues of Construction Materials Laboratory at Kyoto University for their help in experimental works.

REFERENCES

- New Zealand Concrete Design Code Committee. 1976. Proposed Provisions for New Zealand Concrete Design Code, Chapter 22: Prestressed Concrete Members - Additional Seismic Requirements.
- Japan Society of Civil Engineers. 1978. Standard Code for Prestressed Concrete.
- Thompson, K.J. and Park, R. 1980. Ductility of prestressed and partially prestressed concrete beam sections. PCI Jour. 25. No.2:46-70.
- Blakeley, R.W.G. and Park, R. 1973. Prestressed concrete sections with cyclic flexure. Jour. of the Structural Division. 99. No.ST8:1717-1742.